The Journal of Infectious Diseases

MAJOR ARTICLE

Adenylyl Cyclase 6 Expression Is Essential for Cholera Toxin–Induced Diarrhea

Robert A. Fenton,[1] Sathish K. Murali,[1,2] Izumi Kaji,[3,4] Yasutada Akiba,[3,4] Jonathan D. Kaunitz,[3,4] Tina B. Kristensen,[1] Søren B. Poulsen,[1] Jessica A. Dominguez Rieg,[2] and Timo Rieg[2]

[1]Department of Biomedicine, Aarhus University, Denmark; [2]University of South Florida, Tampa; [3]Greater Los Angeles VA Healthcare System, California; and [4]Department of Medicine, University of California, Los Angeles

(See the Editorial commentary by Barrett, on pages 1711–2.)

Background. Cholera toxin (CT)–induced diarrhea is mediated by cyclic adenosine monophosphate (cAMP)–mediated active Cl^- secretion via the cystic fibrosis transmembrane conductance regulator (CFTR). Although the constitutive activation of adenylyl cyclase (AC) in response to CT is due to adenosine diphosphate ribosylation of the small G protein α-subunit activating CFTR with consequent secretory diarrhea, the AC isoform(s) involved remain unknown.

Methods. We generated intestinal epithelial cell–specific adenylyl cyclase 6 (AC6) knockout mice to study its role in CT-induced diarrhea.

Results. AC6 messenger RNA levels were the highest of all 9 membrane-bound AC isoforms in mouse intestinal epithelial cells. Intestinal epithelial-specific AC6 knockout mice ($AC6^{loxloxVillinCre}$) had undetectable AC6 levels in small intestinal and colonic epithelial cells. No significant differences in fluid and food intake, plasma electrolytes, intestinal/colon anatomy and morphology, or fecal water content were observed between genotypes. Nevertheless, CT-induced fluid accumulation in vivo was completely absent in $AC6^{loxloxVillinCre}$ mice, associated with a lack of forskolin- and CT-induced changes in the short-circuit current (I_{SC}) of the intestinal mucosa, impaired cAMP generation in acutely isolated small intestinal epithelial cells, and significantly impaired apical CFTR levels in response to forskolin.

Conclusions. AC6 is a novel target for the treatment of CT-induced diarrhea.

Keywords. adenylyl cyclase; cystic fibrosis; knockout mouse; Ussing chamber; cAMP.

The second most common cause of death worldwide is infectious diarrhea. In developing countries, >20% of children younger than 5 years of age are affected, resulting in approximately 2.5 million deaths per year [1]. One of the major organisms causing infectious diarrhea is *Vibrio cholerae*, a bacterium that produces cholera toxin (CT), which consists of 1 A subunit (enzymatic) and 5 B subunits (required for receptor binding). After the entire toxin complex is endocytosed, the A subunit is cleaved from the rest of the toxin [2, 3]. Subsequently the A subunit moves retrograde in the endoplasmic reticulum and is refolded and released into the cytosol, where it induces adenosine diphosphate (ADP) ribosylation of the small G protein α-subunit, with consequent activation of an unknown adenylyl cyclase (AC) subtype. In vivo and ex vivo studies in mice, rabbits, and rats, as well as in vitro studies conducted in a variety of cell types, showed that CT-induced activation of AC(s) persistently increases cellular cyclic adenosine monophosphate (cAMP) levels [4]. Ultimately, this results in membrane targeting, phosphorylation, and activation of the cystic fibrosis transmembrane regulator (CFTR). These AC-mediated events increase the rate of epithelial Cl^- secretion, which is followed by water secretion, and is the basis of the severe diarrhea [4]. Supporting this mechanism, CFTR knockout mice are partially resistant to CT-induced diarrhea [5] and small molecule CFTR inhibitors reduce fluid secretion in infectious secretory diarrheas [6].

Nine different membrane-bound AC isoforms (AC1–AC9) have been identified [7, 8]. We have examined in detail AC6 function in the kidney: Its high abundance correlates well to its essential contribution to various aspects of renal function, for example, water [9, 10] and electrolyte transport [11, 12] or acid-base homeostasis [13].

Based on the diverse functions of AC6 throughout the body [14], we speculated that AC6 is also important for intestinal function. To study this in isolation, we generated and characterized intestinal-specific AC6 knockout mice and assessed its phenotype with respect to CT-induced diarrhea. The results indicate that AC6 plays a major role in intestinal epithelial cell cAMP generation, CFTR trafficking, and cAMP-induced changes in short-circuit current (I_{SC}). Importantly, intestinal-specific AC6

Received 9 October 2018; editorial decision 4 December 2018; accepted 7 January 2019; published online January 8, 2019.

Presented in part: Experimental Biology, Chicago, Illinois, 22–26 April, 2017. Abstract 703.3.

Correspondence: Timo Rieg, MD, Department of Molecular Pharmacology and Physiology, 12901 Bruce B. Downs Blvd, MDC 08, Tampa, FL 33612 (trieg@health.usf.edu).

The Journal of Infectious Diseases® 2019;220:1719–28

DOI: 10.1093/infdis/jiz013

knockout mice are resistant to CT-induced diarrhea, indicating that AC6 is a potential new target for its rapid treatment.

MATERIALS AND METHODS

Animals

All animal experimentation was conducted in accordance with the Guide for Care and Use of Laboratory Animals (National Institutes of Health) and was approved by the University of South Florida Institutional Animal Care and Use Committee. By crossing transgenic mice in which the *Adcy6* gene is flanked by loxP sites [15] (termed $AC6^{loxlox}$) with mice expressing Cre recombinase under the regulatory element of the villin gene [16], we generated a novel conditional mouse model where AC6 was constitutively deleted only in intestinal epithelial cells (termed $AC6^{loxloxVillinCre}$). Wild-type and $AC6^{-/-}$ mice (on a C57BL/6 background) were reproduced by heterozygote breeding [12]. Primer sequences for genotyping both lines have been previously published [10, 17]. Mice had free access to standard rodent diet (Harlan Teklad 2018) and tap water and were housed under a 12-hour:12-hour light:dark cycle. All experiments were performed on 3- to 6-month-old male mice. Mice of different genotypes, except for experiments where fluid and food intake were measured, were co-housed in the same cages within the facility to limit potential influence of gut microflora on observed phenotypes. The intestinal expression of AC6 was determined in "knock-in" mice ($AC6^{-/-EGFP}$) where enhanced green fluorescent protein (EGFP) is only expressed in AC6-containing cells and thus acts as a surrogate marker of AC6 expression [18]. Labeling of EGFP in paraffin-embedded tissue was performed as previously described [13] using an anti-EGFP antibody (ab6673, Abcam).

Food/Fluid Intake and Blood and Urine Collection/Analysis

Food and fluid intake were determined in regular cages [11, 19]. Blood was collected from the retrobulbar plexus under brief isoflurane anesthesia. Blood chemistry was determined by a blood gas analyzer (OPTIMedical). Fecal water content in freshly defecated stool was calculated as the difference in fresh weight vs dry weight. Fecal dry weight was measured after 24 hours at 80°C.

Sealed Adult Mouse Model

CT- and 8-Br-cAMP–induced [20, 21] diarrhea in mice was performed as described elsewhere. In brief, the anus of mice was occluded with Vetbond (3M) and subsequently mice were gavaged with vehicle (10% sodium bicarbonate [$NaHCO_3$], 0.3% of body weight [BW]), CT (10 μg, Sigma-Aldrich) or 8-Br-cAMP (40 mg/kg BW, Sigma-Aldrich). Mice were euthanized 6 hours after CT or 2 hours after 8-Br-cAMP exposure. Small intestines were removed, weighed, opened to remove the fluid, gently blotted dry, and weighed again. Fluid accumulation ratio was calculated from the ratio of small intestinal weight before fluid removal relative to small intestinal weight after fluid removal.

Morphological and Immunohistochemical Analysis of the Small Intestine and Colon

Small intestines and colons were collected (n = 6/genotype) and measured in length (cm) before flushing fecal contents with ice cold phosphate-buffered saline (PBS) [22, 23]. Tissue was fixed overnight in 4% paraformaldehyde, paraffin embedded, and sectioned at 4–6 μm. Sections were either stained with hematoxylin and eosin, stained for proliferating cell nuclear antigen (1:100; Invitrogen, for proliferation quantification), or stained for cleaved caspase-3 (1:100; Cell Signaling Technology, for apoptosis quantification). Apoptosis and proliferation were determined as described in detail previously [22].

Ussing Chamber Experiments

Mice were euthanized and the terminal ileum approximately 2 cm proximal to the ileocecal junction was removed and opened along the mesenteric border. Under a stereomicroscope, the tunica muscularis was stripped with fine forceps in ice cold Krebs buffer. The mucosa-submucosa preparation was mounted between 2 hemichambers with a 0.3 cm^2 aperture (Physiologic Instruments). Chambers were bathed with serosal Krebs-Ringer solution (117 mmol/L sodium chloride [NaCl], 4.7 mmol/L potassium chloride [KCl], 1.2 mmol/L magnesium chloride [$MgCl_2$], 1.2 mmol/L monosodium phosphate [NaH_2PO_4], 2.5 mmol/L calcium chloride [$CaCl_2$], 25 mmol/L $NaHCO_3$, 11 mmol/L glucose, and 10 μmol/L indomethacin) bubbled with 5% carbon dioxide/95% oxygen (O_2) and luminal Krebs buffer solution (136 mmol/L NaCl, 2.6 mmol/L KCl, 1.8 mmol/L $CaCl_2$, 10 mmol/L HEPES, and 11 mmol/L mannitol, pH 7.4) bubbled with 100% O_2 in a volume of 4 mL each, and maintained at 37°C using a water-recirculating heating system as previously described [24]. The tissues were short-circuited by a voltage clamp (Physiologic Instruments) at zero potential difference with automatic compensation for solution resistance. I_{SC} was measured continuously, with an increase of I_{SC} indicating luminal-to-serosal current flow (eg, anion secretion). The current was recorded by the DataQ system (Physiologic Instruments). The tissues were stabilized for 30 minutes before either the effects of forskolin (1 μmol/L, serosal) or CT (10 μg/mL, mucosal) were investigated.

Isolation of Intestinal Epithelial Cells

Freshly isolated epithelial cells prepared by calcium (Ca^{2+}) chelation [25] are depleted of markers for connective tissue and smooth muscle [26]. In brief, after euthanasia the small intestine and colon were removed, flushed with ice cold PBS, and everted. One end was ligated, and the everted small intestine and colon were filled with Ca^{2+}-free PBS containing 5 mmol/L ethylenediaminetetraacetic acid. The inverted pieces were put in tubes on a rocking platform at 37°C for 15–20 minutes. The tubes were shaken vigorously to release the epithelial cells. After removal of sacs devoid of epithelial cells, tubes were centrifuged

for 2 minutes at 500*g* to pellet the cells. Subsequently, cells were used for further analysis (as detailed below).

Cell Surface Biotinylation

Small intestine jejunal segments were carefully excised and flushed with ice cold PBS. Segments were everted, ligated at one end, filled with Ringer buffer (127 mmol/L NaCl; 10 mmol/L 4-(2-hydroxyethyl)piperazine-1-ethanesulfonic acid, *N*-(2-hydroxyethyl)piperazine-*N′*-(2-ethanesulfonic acid) [HEPES]; 5 mmol/L KCl; 5 mmol/L sodium [Na] pyruvate; 1 mmol/L $MgCl_2$; 5 mmol/L glucose; and 2 mmol/L $CaCl_2$, pH 7.4) and ligated at the other end. Loops were placed in Ringer buffer containing either vehicle, forskolin (1 μmol/L), or 8-Br cAMP (200 μmol/L) for 30 minutes at 37°C. For surface biotinylation, immediately after respective treatments, loops were incubated in ice-cold biotinylation buffer (10 mmol/L triethanolamine, 2 mmol/L $CaCl_2$, and 125 mmol/L NaCl, pH 8.9) containing 1mg/mL EZ-Link Sulfo-NHS-SS-biotin reagent (Life Technologies) for 60 minutes at 4°C. Biotinylated surface proteins were isolated as previously described [27], resolved by sodium dodecyl sulfate–polyacrylamide gel electrophoresis and assessed by immunoblotting. The intracellular proteasome 20S protein was absent from the biotinylated pool, confirming specificity of this fraction for cell surface proteins (not shown).

Immunoblot Analysis

Acutely isolated intestinal epithelial cells were processed for immunoblotting as previously described [26]. Coomassie-stained gels were used to adjust for equal protein loading, with maximal deviations in total protein loading between samples on individual blots ± 10%. Sites of antibody reactivity were detected using enhanced chemiluminescence and signal intensity in specific bands was quantified using Image Studio Lite (Qiagen) densitometry analysis. Antibodies used were AC5/6 (sc-590, Santa Cruz, dilution 1:800), CFTR (ACL-006, Alomone Labs, dilution 1:2500), and anti-actin (A2228, Sigma). For biotin samples, the levels of biotinylated CFTR were normalized to the level of total cellular CFTR in each individual sample.

Reverse-Transcription Quantitative Polymerase Chain Reaction of AC Isoforms and Solute Transporters in Intestinal and Colonic Epithelial Cells

Total RNA from acutely isolated cells was extracted using Trizol reagent (Invitrogen) and reverse-transcription quantitative polymerase chain reaction (RT-qPCR) performed as previously described [28]. Primer sets and efficiency are shown in Supplementary Table 1.

Measurement of cAMP Concentrations in Freshly Isolated Intestinal Epithelial Cells

Enterocyte suspensions were stimulated with forskolin (10 μmol/L; Ascent Scientific), CT (10 μg/mL), or vehicle at 37°C in the presence of 0.5 mmol/L phosphodiesterase inhibitor 3-isobutyl-1-methylxanthine (pretreated for 10 minutes, Sigma-Aldrich). Reactions were terminated after 5 minutes of forskolin stimulation or after 60 minutes for vehicle and CT stimulation by the addition of ice cold 10% TCA (vol/vol). cAMP content was determined by enzyme-linked immunosorbent assay (Direct cAMP ELISA kit, Enzo Life Sciences). Protein concentration was determined using a Pierce protein assay (Thermo Scientific).

Statistical Analysis

Unpaired Student *t* test or Mann–Whitney *U* test was performed as appropriate to analyze for statistical differences between groups. One-way analysis of variance (ANOVA) or 2-way repeated-measures ANOVA followed by Dunnett and Tukey multiple comparison tests, respectively, were used to test for significant differences between genotype and experimental conditions. Significance was considered at $P < .05$.

RESULTS

AC6 Is the Highest Expressed AC Isoform in Intestinal Epithelial Cells

RT-qPCR profiling of acutely isolated small intestinal epithelial cells (IECs) (Figure 1A) or colonic epithelial cells (CECs) (Figure 1B) determined that AC6 is the most abundantly expressed AC isoform. AC6 expression levels were approximately 10- to 1000-fold higher than any of the other AC isoforms, with a variable profile between IECs or CECs. Our unpublished observations indicated that commercial AC6 antibodies are unsuitable for immunolabeling; we thus confirmed that AC6 was only expressed in intestinal epithelial cells by examining AC6 expression patterns using $AC6^{-/-}$EGFP mice. In these mice, EGFP expression is a surrogate marker of AC6 expression [18]. Immunolabeling for EGFP was undetectable in sections from control mice (Figure 1C), whereas EGFP was strongly expressed in epithelial cells of the small intestine and colon in $AC6^{-/-}$EGFP mice (Figure 1C).

Lack of AC6 in the Intestine Is Not Associated With Physiological Abnormalities

To study the physiological function of intestinal AC6, we generated a novel mouse model where AC6 was selectively deleted from intestinal epithelial cells using Cre recombinase under control of the the villin promoter ($AC6^{loxloxVilllinCre}$). $AC6^{loxloxVillinCre}$ mice were born at predicted Mendelian frequencies, appeared grossly indistinguishable from control ($AC6^{loxlox}$) mice, and developed normally. Confirming the model, messenger RNA (mRNA) and protein (Figure 1D and 1E) levels of AC6 in $AC6^{loxloxVilllinCre}$ mice were virtually undetectable in isolated IECs or CECs. Intestinal morphology in $AC6^{loxloxVillinCre}$ mice was largely normal (Supplementary Figure 1), with the overall length of the small intestine and colon (Figure 2A) and individual villus length and crypt depth not significantly different from control mice (Figure 2B). Quantification of epithelial cell proliferation (Figure 2C) and

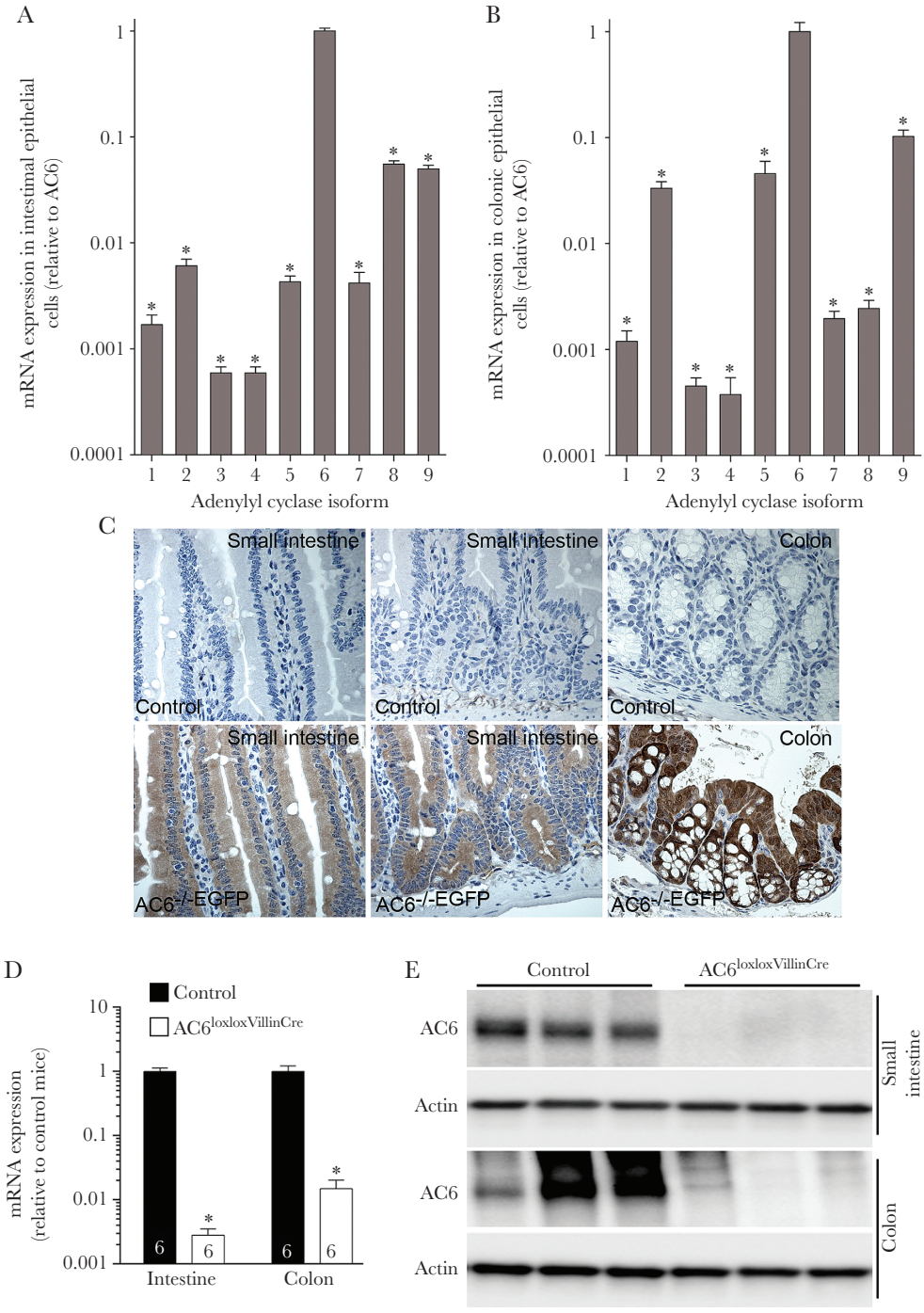

Figure 1. Intestinal epithelial cell–specific adenylyl cyclase 6 (AC6) knockout mice. Messenger RNA (mRNA) expression of AC isoforms (1–9) in epithelial cells isolated from the small intestine (*A*) or colon (*B*) of $AC6^{loxlox}$ mice (n = 5). Data were analyzed by 1-way analysis of variance followed by Dunnett multiple comparison test. **P* < .0001 relative to AC6. *C*, Representative immunohistochemistry images from $AC6^{-/-EGFP}$ mouse intestine stained with an anti–enhanced green fluorescent protein (EGFP) antibody (n = 4/genotype). EGFP (surrogate marker of AC6 expression) was observed in all epithelial cells of the small intestine and colon. *D*, mRNA expression of AC6 in epithelial cells isolated from the intestine or colon of control ($AC6^{loxlox}$) or $AC6^{loxloxVillinCre}$ mice (numbers refer to 'n'). Data were analyzed by an unpaired Student *t* test. **P* < .005 relative to control. *E*, AC6 protein was virtually undetectable in epithelial cells isolated from the small intestine or colon of $AC6^{loxloxVillinCre}$ mice. Data are expressed as mean ± standard error of the mean.

apoptosis (Figure 2D and 2E) was indistinguishable between genotypes. Under baseline conditions, fecal water content was similar between $AC6^{loxloxVillinCre}$ mice and controls (Figure 2F). Further physiological characterization did not show any significant differences in BW; fluid and food intake; plasma Na^+, K^+, Ca^{2+}, phosphate, and H^+ concentrations; or hematocrit (Figure

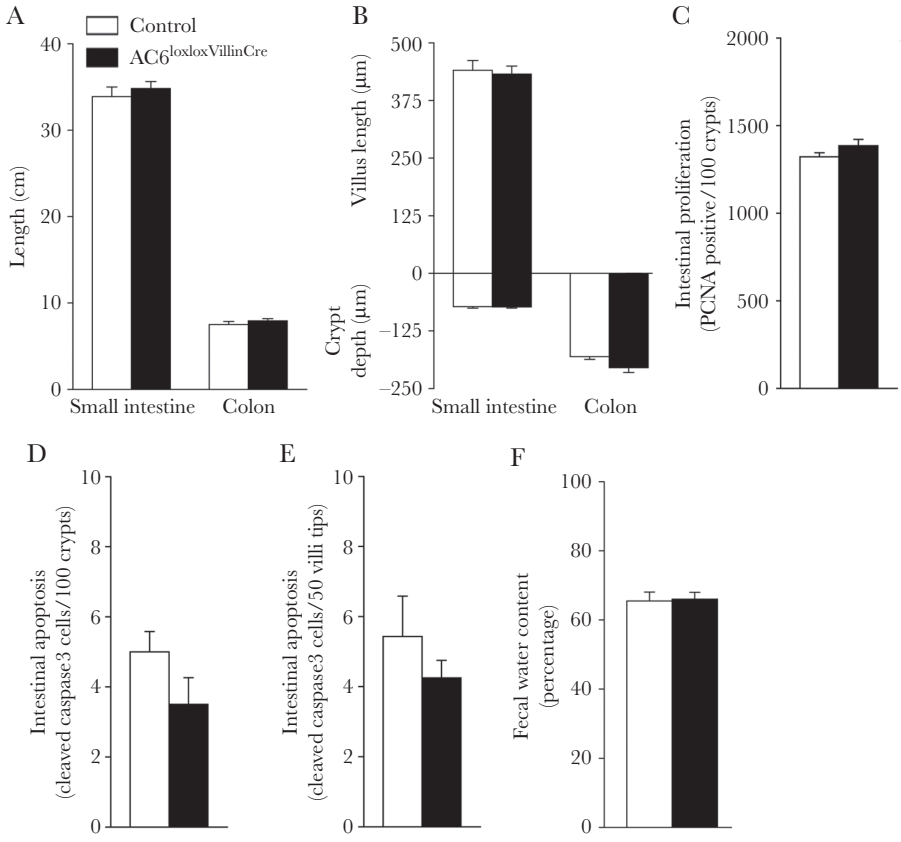

Figure 2. Normal intestinal morphology in the absence of adenylyl cyclase 6 (AC6) in intestinal epithelial cells. *A*, Length of the small intestine and colon is comparable between genotypes (n = 6/genotype). *B*, Villus length and crypt depth is not significantly different between genotypes (n = 6/genotype). *C–F*, Intestinal proliferation and apoptosis were not significantly different between genotypes (n = 6/genotype). *G*, Fecal water content was comparable between genotypes (n = 6/genotype). Data were analyzed by an unpaired Student *t* test and are expressed as mean ± standard error of the mean. Abbreviations: AC, adenylyl cyclase; PCNA, proliferating cell nuclear antigen.

3A–H). RT-qPCR profiling of isolated IECs or CECs for major transport proteins important for maintaining body electrolyte homeostasis revealed minor differences. In the small intestine, glucose transporter (GLUT) 2, GLUT5, and CFTR levels were significantly lower in AC6^{loxloxVillinCre} relative to control mice (Figure 3I), whereas in the colon levels of the α- and β-subunits of the epithelial sodium channel (ENaC) and CFTR were significantly lower.

Lack of AC6 Does Not Affect Baseline I_{sc} but Mediates CT-Induced Changes in I_{sc}

Ussing chamber experiments conducted on acutely isolated small intestinal mucosa showed no differences in I_{SC} under baseline conditions (Figure 4A). The nonselective activator of adenylyl cyclases, forskolin, converts intestinal Cl^- absorption into secretion [2], which can be measured by changes in I_{SC}. Serosal addition of forskolin to the small intestinal mucosa isolated from control mice caused a rapid increase, followed by sustained elevation in I_{SC}, whereas no response was observed in mucosa isolated from AC6^{loxloxVillinCre} (representative traces in Figure 4B). I_{SC} increased approximately 35 μA/cm^2 in response to forskolin in control mice, whereas the response in AC6^{loxloxVillinCre} mice was completely absent (Figure 4C). In similar experiments, I_{SC} was increased in small intestinal mucosa from control mice in response to luminal CT (representative traces in Figure 4D, summary data in Figure 4E). In comparison to forskolin-induced changes in I_{SC}, the effects of CT took on average 1 hour to develop, possibly as a consequence of CT endocytosis and the involved CFTR trafficking events required for CT action. The increased I_{SC} observed in control mice (~40 μA/cm^2) in response to CT was completely absent in AC6^{loxloxVillinCre} mice (Figure 4D and 4E). The I_{SC} response observed in AC6^{loxloxVillinCre} was similar to that observed in AC6$^{-/-}$ mice, although the small number of AC6$^{-/-}$ mice examined prevents solid conclusions being drawn from this data.

AC6 Mediates In Vivo Fluid Accumulation in Response to CT

The "sealed" adult mouse model [20] was utilized to determine if CT-induced fluid secretion is mediated by AC6 in vivo. In control mice, oral gavage of CT increased the fluid accumulation ratio in the small intestine by approximately 1.5-fold compared to vehicle treatment (Figure 5A). CT-induced fluid accumulation was completely absent from AC6^{loxloxVillinCre} and AC6$^{-/-}$ mice (Figure 5A). In contrast, similar experiments performed using the cell-permeable cAMP

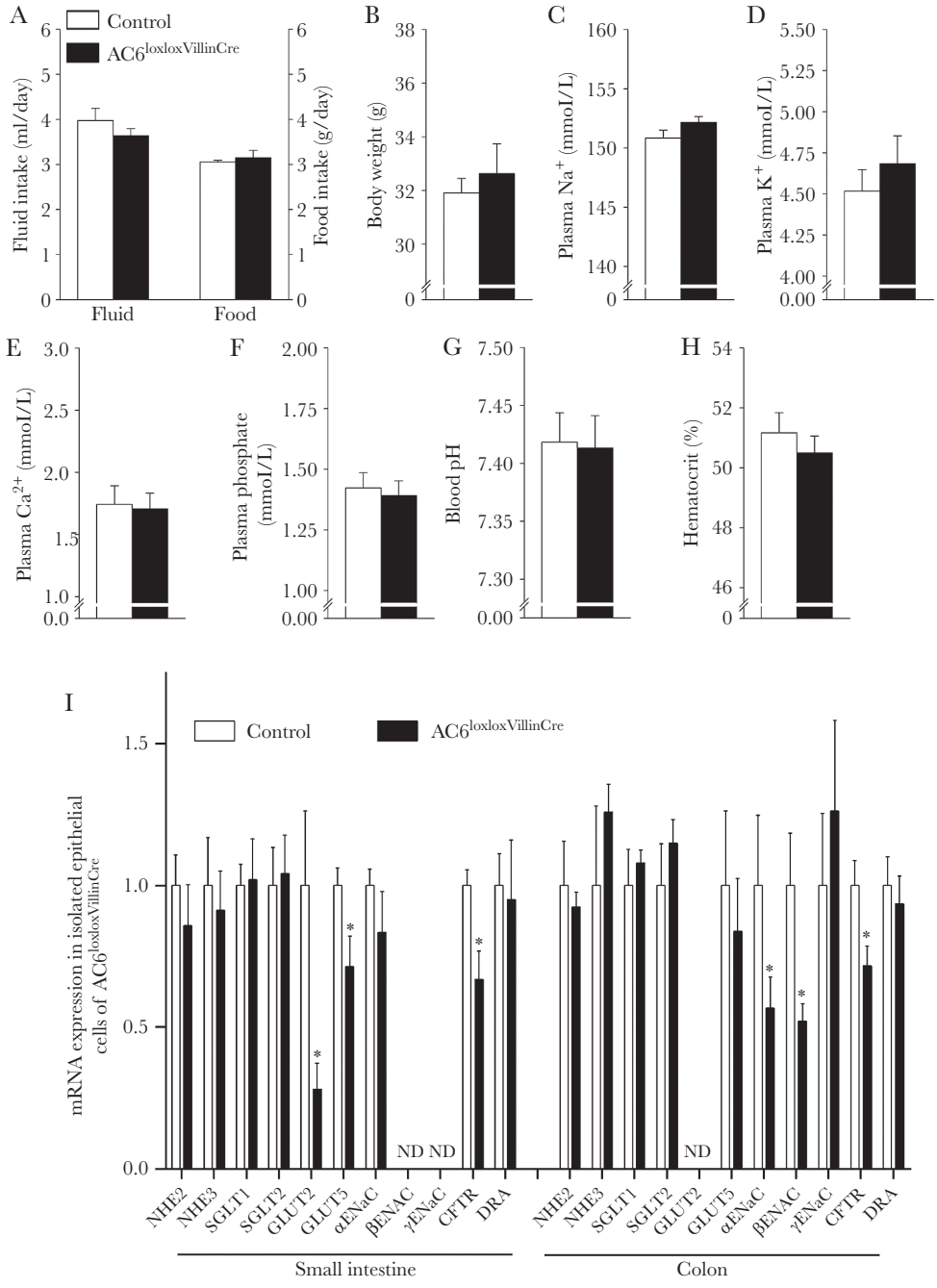

Figure 3. Lack of adenylyl cyclase 6 (AC6) in intestinal epithelial cells is not associated with an overt phenotype. Physiological analysis of control ($AC6^{loxlox}$) and $AC6^{loxloxVillinCre}$ mice with free access to food and water in regular cages (averaged over a 6-day period). No significant differences between the genotypes were observed for fluid or food intake (*A*; note the use of 2 y-axes), body weight (*B*), plasma Na^+ (*C*), plasma K^+ (*D*), plasma Ca^{2+} (*E*), plasma phosphate (*F*), blood pH (*G*), or hematocrit (*H*) (n = 6/genotype). *I*, Messenger RNA (mRNA) expression of various transporters and channels in epithelial cells isolated from the small intestine or colon of control ($AC6^{loxlox}$) or $AC6^{loxloxVillinCre}$ mice (n = 5/genotype). See Supplementary Table 1 for additional nomenclature details. ND = not detectable. All data were analyzed by unpaired Student *t* test; $^*P < .05$ relative to control. Data are expressed as mean ± standard error of the mean.

analogue 8-Br-cAMP increased small intestinal fluid accumulation in $AC6^{loxloxVillinCre}$ mice to similar levels as present in control mice in response to CT (Figure 5B), indicating that the lack of response to CT in $AC6^{loxloxVillinCre}$ is not due to a generalized dysfunction of the intestinal mucosa or differences in CFTR expression/function.

AC6 is Essential for CT-Induced Increases in cAMP and CFTR Membrane Accumulation

CT increases intracellular cAMP levels in enterocytes [4]. To address whether the lack of CT-induced increases in I_{SC} or intestinal fluid accumulation in $AC6^{loxloxVillinCre}$ are due to alterations in cAMP levels, the effects of CT or forskolin on acutely

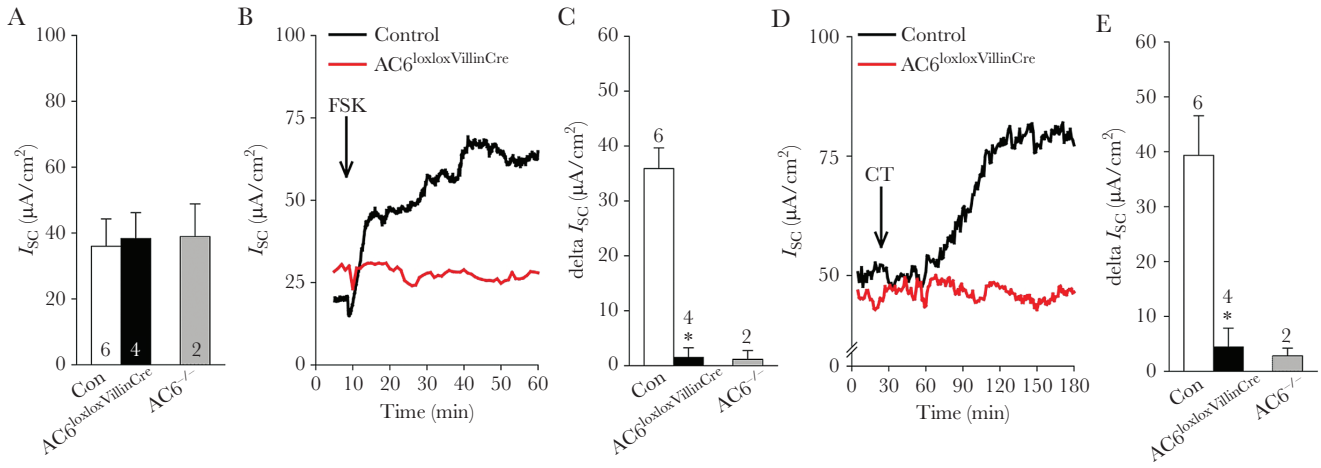

Figure 4. Adenylyl cyclase 6 (AC6) mediates forskolin (FSK) and cholera toxin (CT)–induced changes in short-circuit current (*ISC*) in intestinal mucosa. *A*, Ussing chamber experiments on small intestinal mucosa indicated that baseline *ISC* was not significantly different among control (Con, AC6^{loxlox}) and AC6^{loxloxVillinCre} mice. Data from a limited number of AC6$^{-/-}$ mice were also included as a comparison, but a statistical analysis of this data is excluded due to small number of observations. *B*, Representative traces of the effects of mucosal FSK (1 μmol/L) on *ISC* in control and AC6^{loxloxVillinCre} mice. *C*, Summary of the FSK-induced changes in *ISC* in control and AC6^{loxloxVillinCre} mice. *D*, Representative traces of the effects of luminal CT (10 μg/mL) on *ISC* in control and AC6^{loxloxVillinCre} mice. *E*, Summary of the CT-induced changes in *ISC* in control and AC6^{loxloxVillinCre} mice. Numbers associated to individual bars represent sample size "n." Data were analyzed by unpaired Student *t* test. **P* < .05 vs control. Data are expressed as mean ± standard error of the mean, except for AC6$^{-/-}$ mice (expressed as mean ± standard deviation).

isolated IECs was examined. In IECs from control mice, both CT and forskolin significantly (4- to 6-fold) increased cAMP levels (Figure 5C). In contrast, in IECs acutely isolated from AC6^{loxloxVillinCre} mice, CT had no significant effect on cAMP levels, whereas forskolin only a minor effect (Figure 5C). To investigate the basis for this forskolin response the expression levels of other adenylyl cyclase isoforms in AC6^{loxloxVillinCre} mice was measured using RT-qPCR. In IECs of AC6^{loxloxVillinCre} mice, AC1, AC4, and AC8 levels were lower, but AC3 levels were higher compared to control mice (Figure 5D). In CECs from AC6^{loxloxVillinCre} mice, AC8 expression was significantly lower, whereas AC2, AC3, and AC7 levels were significantly higher (Figure 5E). Under normal conditions, the increased cAMP levels due to CT-induced protein kinase A activity increase CFTR phosphorylation with consequent increased Cl^- channel open probability and CFTR cell surface stability [29]. To examine the latter condition, small intestinal loops from control, AC6^{loxloxVillinCre}, and AC6$^{-/-}$ mice were biotinylated from the mucosal side ex vivo, and the levels of CFTR in the biotinylated fraction, relative to the total cellular levels of CFTR, were examined. Under baseline conditions, relative CFTR surface expression was not significantly different between genotypes (Figure 5F and 5G). Forskolin increased CFTR levels in the biotinylated pool of control animals approximately 2-fold, whereas it had no significant effects on relative CFTR surface expression in AC6^{loxloxVillinCre} and AC6$^{-/-}$ mice. In contrast, direct activation of cAMP-dependent signaling pathways using 8-Br-cAMP increased relative CFTR surface expression equally in all genotypes (Figure 5F and 5G), indicating that CFTR trafficking is fully functional in the AC6 gene-modified mice.

DISCUSSION

In developed countries, secretory diarrhea is a frequent cause of physician visits and hospitalization, and current therapies such as fluid and electrolyte replacement or antibiotic treatment are often only partially effective in children and/or do not result in short-term cessation of symptoms [30, 31]. Therefore, identifying the underlying mechanisms of secretory diarrhea is essential to developing new strategies for rapid treatment of this condition. One of the major organisms implicated in the pathogenesis of secretory diarrhea is the cholera enterotoxin (CT). The major finding in this study is that in mice, intestinal epithelial cell AC6 activity is an essential component of the mechanism whereby CT causes secretory diarrhea, suggesting that selectively inhibiting AC6 would be a novel and promising avenue for pharmaceutical development to rapidly treat the secretory diarrhea associated with cholera infection.

Of the 9 membrane-bound adenylyl cyclases expressed in mouse intestinal epithelial cells, AC6 was the most abundant, suggesting a major functional relevance. To selectively assess AC6 only in intestinal epithelial cells, we generated a mouse model based on villin promoter-driven cre recombinase expression [16]. In this model AC6 was absent from the small intestine, and virtually undetectable in colon, matching endogenous expression of the villin gene used to drive cre recombinase expression [32]. Furthermore, although villin is expressed in the kidney proximal tubule [33], we saw no consistent evidence for cre recombinase expression in kidneys from our AC6^{loxloxVillinCre} mice (data not shown), consistent with previous studies [16] and highlighting that the villin-driven cre expression is likely

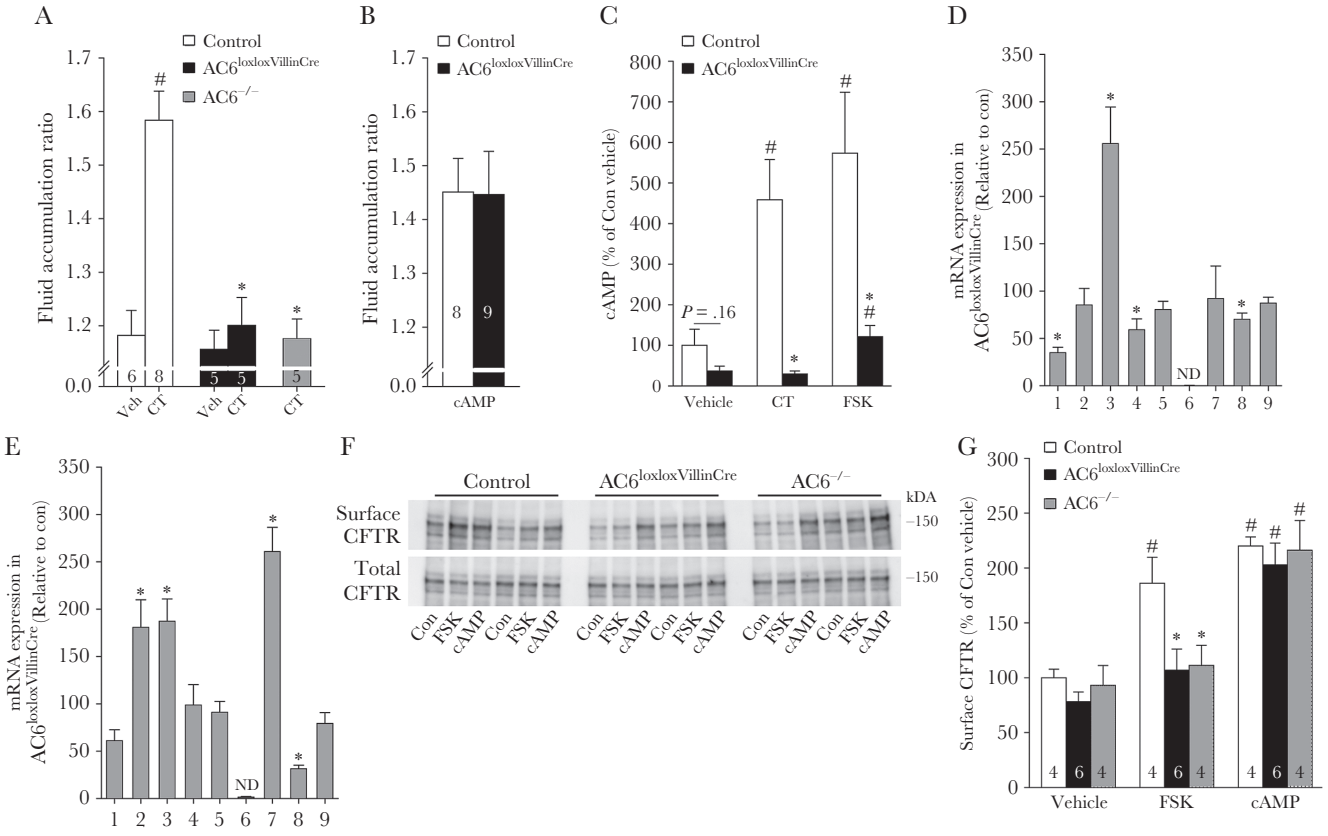

Figure 5. The effects of cholera toxin (CT) in vivo are mediated by adenylyl cyclase 6 (AC6). *A*, In the adult "sealed" mouse model, CT (10 µg/mouse) induced a significant increase in intestinal fluid accumulation in control (con, $AC6^{loxlox}$), but not $AC6^{loxloxVillinCre}$ and $AC6^{-/-}$ mice. Data were analyzed by 1-way analysis of variance (ANOVA) followed by Tukey multiple comparison test. $^{\#}P < .05$ CT vs vehicle within genotype. $^{*}P < .05$ between control and gene-modified mice within a treatment group. *B*, Fluid accumulation in control and $AC6^{loxloxVillinCre}$ mice could be stimulated to a similar degree using 8-Br–cyclic adenosine monophosphate (cAMP, 40 mg/kg). Data were analyzed by unpaired Student *t* test. *C*, In isolated intestinal epithelial cells from control mice (n = 4), forskolin (FSK, 1 µmol/L) or CT (10 µg/mL) significantly increased cAMP levels. Stimulation of cAMP formation by CT was completely absent and the response to FSK was severely attenuated in $AC6^{loxloxVillinCre}$ mice (n = 4). Data were analyzed by 1-way ANOVA followed by Tukey multiple comparison test. $^{\#}P < .05$ treatment vs vehicle within genotype. $^{\#}P < .05$ between control and gene-modified mice within a treatment group. $^{*}P < .05$ relative to control mice. *D*, Relative messenger RNA (mRNA) expression levels of adenylyl cyclases in epithelial cells isolated from the intestine or colon (*E*) of control or $AC6^{loxloxVillinCre}$ mice (n = 5/genotype). ND = not detectable. Data were analyzed by unpaired Student *t* test. $^{*}P < .05$ relative to control mice. *F*, Representative immunoblot of biotinylated (surface) and total cellular cystic fibrosis transmembrane conductance regulator (CFTR) levels in enterocytes isolated from control, $AC6^{loxloxVilinCre}$, and $AC6^{-/-}$ mice following FSK (1 µmol/L) or 8-Br-cAMP (10 mmol/L) treatment. Each lane represents a sample from an individual mouse and shows the surface CFTR and total CFTR within the same preparation. *G*, Summary of ex vivo biotinylation studies. CTFR surface levels, relative to total CFTR levels within the same sample, were not different between genotypes upon vehicle application. FSK significantly increased surface CFTR in control but not genetically modified mice, whereas 8-Br-cAMP increased surface CFTR levels in $AC6^{loxloxVillinCre}$ and $AC6^{-/-}$ mice to levels observed in control mice. Numbers associated to individual bars represent sample size "n." Data were analyzed by 1-way ANOVA followed by Tukey multiple comparison test. $^{\#}P < .05$ treatment vs vehicle within genotype. $^{*}P < .05$ between control and gene-modified mice within a treatment group. Data are expressed as mean ± standard error of the mean.

sensitive to organ-specific positional effects [32]. In line with AC6 being the major mediator of cAMP production in intestinal epithelial cells, forskolin-induced increases in cAMP were severely attenuated in intestinal epithelial cells isolated from $AC6^{loxloxVillinCre}$ mice. These alterations in cAMP could not be fully compensated for by 2- to 3-fold increases in other adenylyl cyclase isoforms, and are likely responsible for the observed reduction in cAMP-responsive GLUT2, GLUT5, and α/β-ENaC [34]. Despite this, under nonstressed conditions, $AC6^{loxloxVillinCre}$ mice had normal physiology. Therefore, either (*i*) other signaling pathways must play an important role under baseline conditions, (*ii*) compensatory signaling pathways such as the Ca^{2+} pathway could exist to modulate electrolyte transport pathways in the $AC6^{loxloxVillinCre}$ mice, or (*iii*) the basal levels of cAMP in the $AC6^{loxloxVillinCre}$ mice model are sufficient to maintain normal intestinal ion and water transport. The latter possibility is supported by the relatively normal I_{SC} measurements in isolated mucosa from $AC6^{-/-}$ or $AC6^{loxloxVillinCre}$ mice under baseline conditions.

Fluid secretion by the mammalian intestine following CT involves osmotic water movement into the intestinal lumen subsequent to increased transepithelial Cl^- secretion via CFTR [2]. The central finding of this study is that cAMP production via AC6 is essential for this process and is supported by (*i*) a lack of change in I_{SC} in mucosa isolated from $AC6^{loxloxVillinCre}$ mice subsequent to CT treatment (indicating no net change in

ion transport), and (*ii*) a complete absence of CT-induced fluid accumulation in AC6^{loxloxVillinCre} and AC6$^{-/-}$ mice. Therefore, although other hormones and paracrine signaling molecules have been speculated to be involved in CT-induced effects, for example, serotonin [35] or prostaglandins [36] (partly excluded by our Ussing chamber results performed in the presence of a cyclooxygenase inhibitor), none of them can exert substantial effects in the absence of AC6.

Based on our results, pharmacological inhibition of AC6 by small molecules should be beneficial for rapid relief of CT-induced diarrhea. Although several previous strategies to alleviate the effects of CT have been proposed [37, 38], including inhibition of CFTR using small molecules [6, 39] or neutralization of cholera toxin with nanoparticle decoys [40], these approaches could be limited by potential cellular toxicity, biocompatibility, or cost-ineffective manufacturing. As AC6^{loxloxVillinCre} mice did not present with altered epithelial cell integrity or morphology and whole body deletion of AC6 does not result in a major deleterious phenotype, targeting AC6 may even have distinct advantages to these other approaches for treatment of CT-induced secretory diarrhea. However, development of drugs against membrane-bound ACs has been limited and currently there are no selective membrane-permeable inhibitors of AC6 or clinically useful AC inhibitors in general [7]. Conversely, further work to determine if activation of AC6 may be beneficial to stimulate fluid secretion and treat certain forms of constipation would be informative, but currently specific activators of different AC isoforms are not available.

Supplementary Data

Supplementary materials are available at *The Journal of Infectious Diseases* online. Consisting of data provided by the authors to benefit the reader, the posted materials are not copyedited and are the sole responsibility of the authors, so questions or comments should be addressed to the corresponding author.

Notes

Author contributions. R. A. F., J. D. R., and T. R. conceived and designed the work. All animal experiments were performed in the laboratory of T. R., R. A. F., S. B. P., J. D. R., S. K. M,, I. K., Y. A., J. D. K., and T. R. contributed to the acquisition, analysis, or interpretation of data for the work. T. R. and R. A. F. drafted the work. All authors approved the final version of the manuscript; agree to be accountable for all aspects of the work in ensuring that questions related to the accuracy or integrity of any part of the work are appropriately investigated and resolved; and confirm that all persons designated as authors qualify for authorship and all those who qualify for authorship are listed.

Financial support. This work was supported by the National Institute of Diabetes and Digestive and Kidney Diseases (grant numbers R01DK110621 to T. R. and R01DK54221 to J. D. K.). Funding (to R. A. F) was also provided by the Lundbeckfonden, the Danish Council for Independent Research, and the Novo Nordisk Fonden. The work was further supported by the U.S. Department of Veterans Affairs 5I01BX001245 to J. D. K.

Potential conflicts of interest. All authors: No reported conflicts of interest. All authors have submitted the ICMJE Form for Disclosure of Potential Conflicts of Interest. Conflicts that the editors consider relevant to the content of the manuscript have been disclosed.

References

1. Kassebaum N, Kyu HH, Zoeckler L, et al; Global Burden of Disease Child and Adolescent Health Collaboration. Child and adolescent health from 1990 to 2015: findings from the Global Burden of Diseases, Injuries, and Risk Factors 2015 study. JAMA Pediatr **2017**; 171:573–92.
2. Barrett KE, Keely SJ. Chloride secretion by the intestinal epithelium: molecular basis and regulatory aspects. Annu Rev Physiol **2000**; 62:535–72.
3. Lencer WI, Moe S, Rufo PA, Madara JL. Transcytosis of cholera toxin subunits across model human intestinal epithelia. Proc Natl Acad Sci U S A **1995**; 92:10094–8.
4. Field M. Intestinal ion transport and the pathophysiology of diarrhea. J Clin Invest **2003**; 111:931–43.
5. Gabriel SE, Brigman KN, Koller BH, Boucher RC, Stutts MJ. Cystic fibrosis heterozygote resistance to cholera toxin in the cystic fibrosis mouse model. Science **1994**; 266:107–9.
6. Thiagarajah JR, Broadbent T, Hsieh E, Verkman AS. Prevention of toxin-induced intestinal ion and fluid secretion by a small-molecule CFTR inhibitor. Gastroenterology **2004**; 126:511–9.
7. Dessauer CW, Watts VJ, Ostrom RS, Conti M, Dove S, Seifert R. International union of basic and clinical pharmacology. CI. structures and small molecule modulators of mammalian adenylyl cyclases. Pharmacol Rev **2017**; 69:93–139.
8. Steegborn C. Structure, mechanism, and regulation of soluble adenylyl cyclases—similarities and differences to transmembrane adenylyl cyclases. Biochim Biophys Acta **2014**; 1842:2535–47.
9. Rieg T, Tang T, Murray F, et al. Adenylate cyclase 6 determines cAMP formation and aquaporin-2 phosphorylation and trafficking in inner medulla. J Am Soc Nephrol **2010**; 21:2059–68.
10. Poulsen SB, Kristensen TB, Brooks HL, Kohan DE, Rieg T, Fenton RA. Role of adenylyl cyclase 6 in the development of lithium-induced nephrogenic diabetes insipidus. JCI Insight **2017**; 2:e91042.
11. Fenton RA, Murray F, Dominguez Rieg JA, Tang T, Levi M, Rieg T. Renal phosphate wasting in the absence of adenylyl cyclase 6. J Am Soc Nephrol **2014**; 25:2822–34.
12. Rieg T, Tang T, Uchida S, Hammond HK, Fenton RA, Vallon V. Adenylyl cyclase 6 enhances NKCC2 expression

and mediates vasopressin-induced phosphorylation of NKCC2 and NCC. Am J Pathol **2013**; 182:96–106.
13. Poulsen SB, Marin De Evsikova C, Murali SK, et al. Adenylyl cyclase 6 is required for maintaining acid-base homeostasis. Clin Sci (Lond) **2018**; 132:1779–96.
14. Defer N, Best-Belpomme M, Hanoune J. Tissue specificity and physiological relevance of various isoforms of adenylyl cyclase. Am J Physiol Renal Physiol **2000**; 279:F400–16.
15. Roos KP, Strait KA, Raphael KL, Blount MA, Kohan DE. Collecting duct-specific knockout of adenylyl cyclase type VI causes a urinary concentration defect in mice. Am J Physiol Renal Physiol **2012**; 302:F78–84.
16. Madison BB, Dunbar L, Qiao XT, Braunstein K, Braunstein E, Gumucio DL. Cis elements of the villin gene control expression in restricted domains of the vertical (crypt) and horizontal (duodenum, cecum) axes of the intestine. J Biol Chem **2002**; 277:33275–83.
17. Fenton RA, Poulsen SB, de la Mora Chavez S, Soleimani M, Dominguez Rieg JA, Rieg T. Renal tubular NHE3 is required in the maintenance of water and sodium chloride homeostasis. Kidney Int **2017**; 92:397–414.
18. Chien CL, Wu YS, Lai HL, et al. Impaired water reabsorption in mice deficient in the type VI adenylyl cyclase (AC6). FEBS Lett **2010**; 584:2883–90.
19. Fenton RA, Poulsen SB, de la Mora Chavez S, et al. Caffeine-induced diuresis and natriuresis is independent of renal tubular NHE3. Am J Physiol Renal Physiol **2015**; 308:F1409–20.
20. Richardson SH, Giles JC, Kruger KS. Sealed adult mice: new model for enterotoxin evaluation. Infect Immun **1984**; 43:482–6.
21. Giannella RA, Drake KW. Effect of purified *Escherichia coli* heat-stable enterotoxin on intestinal cyclic nucleotide metabolism and fluid secretion. Infect Immun **1979**; 24:19–23.
22. Dominguez Rieg JA, Chirasani VR, Koepsell H, Senapati S, Mahata SK, Rieg T. Regulation of intestinal SGLT1 by catestatin in hyperleptinemic type 2 diabetic mice. Lab Invest **2016**; 96:98–111.
23. Khailova L, Frank DN, Dominguez JA, Wischmeyer PE. Probiotic administration reduces mortality and improves intestinal epithelial homeostasis in experimental sepsis. Anesthesiology **2013**; 119:166–77.
24. Kaji I, Akiba Y, Kato I, Maruta K, Kuwahara A, Kaunitz JD. Xenin augments duodenal anion secretion via activation of afferent neural pathways. J Pharmacol Exp Ther **2017**; 361:151–61.
25. Zeineldin M, Neufeld K. Isolation of epithelial cells from mouse gastrointestinal tract for Western blot or RNA analysis. Bio Protoc **2012**; 2:e292.
26. Yde J, Keely S, Wu Q, et al. Characterization of AQPs in mouse, rat, and human colon and their selective regulation by bile acids. Front Nutr **2016**; 3:46.
27. Rosenbaek LL, Rizzo F, Wu Q, et al. The thiazide sensitive sodium chloride co-transporter NCC is modulated by site-specific ubiquitylation. Sci Rep **2017**; 7:12981.
28. Wu Q, Moeller HB, Stevens DA, et al. CHIP regulates aquaporin-2 quality control and body water homeostasis. J Am Soc Nephrol **2018**; 29:936–48.
29. Chin S, Hung M, Bear CE. Current insights into the role of PKA phosphorylation in CFTR channel activity and the pharmacological rescue of cystic fibrosis disease-causing mutants. Cell Mol Life Sci **2017**; 74:57–66.
30. Binder HJ, Brown I, Ramakrishna BS, Young GP. Oral rehydration therapy in the second decade of the twenty-first century. Curr Gastroenterol Rep **2014**; 16:376.
31. Thiagarajah JR, Donowitz M, Verkman AS. Secretory diarrhoea: mechanisms and emerging therapies. Nat Rev Gastroenterol Hepatol **2015**; 12:446–57.
32. Pinto D, Robine S, Jaisser F, El Marjou FE, Louvard D. Regulatory sequences of the mouse villin gene that efficiently drive transgenic expression in immature and differentiated epithelial cells of small and large intestines. J Biol Chem **1999**; 274:6476–82.
33. Maunoury R, Robine S, Pringault E, Léonard N, Gaillard JA, Louvard D. Developmental regulation of villin gene expression in the epithelial cell lineages of mouse digestive and urogenital tracts. Development **1992**; 115:717–28.
34. Gouyon F, Onesto C, Dalet V, Pages G, Leturque A, Brot-Laroche E. Fructose modulates GLUT5 mRNA stability in differentiated Caco-2 cells: role of cAMP-signalling pathway and PABP (polyadenylated-binding protein)-interacting protein (Paip) 2. Biochem J **2003**; 375:167–74.
35. Turvill JL, Connor P, Farthing MJ. The inhibition of cholera toxin-induced 5-HT release by the 5-HT(3) receptor antagonist, granisetron, in the rat. Br J Pharmacol **2000**; 130:1031–6.
36. Peterson JW, Ochoa LG. Role of prostaglandins and cAMP in the secretory effects of cholera toxin. Science **1989**; 245:857–9.
37. Thiagarajah JR, Verkman AS. New drug targets for cholera therapy. Trends Pharmacol Sci **2005**; 26:172–5.
38. Muanprasat C, Chatsudthipong V. Cholera: pathophysiology and emerging therapeutic targets. Future Med Chem **2013**; 5:781–98.
39. Cil O, Phuan PW, Gillespie AM, et al. Benzopyrimido-pyrrolo-oxazine-dione CFTR inhibitor ®-BPO-27 for antisecretory therapy of diarrheas caused by bacterial enterotoxins. FASEB J **2017**; 31:751–60.
40. Das S, Angsantikul P, Le C, et al. Neutralization of cholera toxin with nanoparticle decoys for treatment of cholera. PLoS Negl Trop Dis **2018**; 12:e0006266.